Ecology, 90(8), 2009, pp. 2190–2201

Nitrogen fixation in different biogeochemical niches along a 120 000-year chronosequence in New Zealand

Duncan N. L. Menge[1] and Lars O. Hedin

Department of Ecology and Evolutionary Biology, Princeton University, Princeton, New Jersey 08544 USA

Abstract. Biological nitrogen fixation (BNF) is the major nitrogen (N) input in many terrestrial ecosystems, yet we know little about the mechanisms and feedbacks that control this process in natural ecosystems. We here examine BNF in four taxonomically and ecologically different groups over the course of forest ecosystem development. At nine sites along the Franz Josef soil chronosequence (South Westland, New Zealand) that range in age from 7 to 120 000 yr old, we quantified BNF from the symbiotic plant *Coriaria arborea*, cyanolichens (primarily *Pseudocyphellaria* spp.), bryophytes (many species), and heterotrophic bacteria in leaf litter. We specifically examined whether these groups could act as "nitrostats" at the ecosystem level, turning BNF on when N is scarce (early in primary succession) and off when N is plentiful (later in succession and retrogression). *Coriaria* was abundant and actively fixing ($\sim$11 kg N·ha^{-1}·yr^{-1}) in the youngest and most N-poor site (7 yr old), consistent with nitrostat dynamics. *Coriaria* maintained high BNF rates independent of soil N availability, however, until it was excluded from the community after a single generation. We infer that *Coriaria* is an obligate N fixer and that the nitrostat feedback is mechanistically governed by species replacement at the community level, rather than down-regulation of BNF at the physiological scale. Biological nitrogen fixation inputs from lichens (means of 0–2 kg N·ha^{-1}·yr^{-1}), bryophytes (0.7–10 kg N·ha^{-1}·yr^{-1}), and litter (1–2 kg N·ha^{-1}·yr^{-1}) were driven primarily by changes in density, which peaked at intermediate-aged sites (and increased with soil N availability) for both lichens and bryophytes, and grew monotonically with soil age (but did not change with soil N) for litter. This non-nitrostatic link between soil N availability and lichen/bryophyte BNF likely stems from increased tree biomass in more fertile sites, which increases epiphytic moisture conditions and habitable surface area. This apparent positive feedback could produce N-rich conditions.

Key words: *bryophyte;* Coriaria arborea; *ecosystem development; feedback; Franz Josef, New Zealand; leaf litter; lichen; nitrostat; primary succession;* Pseudocyphellaria.

Introduction

Nutrients play a key role in forest development. Nitrogen (N) is typically in short supply early in primary succession (decades to centuries) because there is usually little N in rock, but it accumulates over time due to inputs from the atmosphere and biological N fixation (BNF). In contrast, phosphorus (P) is relatively plentiful early in succession due to weathering of abundant P-containing minerals (such as apatite), but in the absence of disturbance, P becomes more scarce over ecosystem development timescales (millennia to millions of years) as the weathering source is depleted (Walker and Syers 1976, Hedin et al. 2003, Vitousek 2004).

Biological N fixation is of particular importance for this conceptual model, in part because it can bring in large amounts of external N into an ecosystem (at rates of 50 kg N·ha^{-1}·yr^{-1} or more in some systems [e.g., Binkley et al. 1992, Uliassi and Ruess 2002]). Importantly, in the same way as a thermostat turns a heater on when a room is too cold, BNF may act as a "nitrostat," turning on when N is limiting and turning off when it is not (because BNF is thought to be energetically costly relative to soil N uptake [Gutschick 1981]). This biological regulation could bring an ecosystem out of N limitation and thus feed back upon the availability and dynamics of nutrients over the course of succession and ecosystem development.

From the perspective of a spatially homogeneous model ecosystem, in which biologically available N in the soil can be taken as an ecosystem-level indicator of N status, a perfect nitrostat would turn BNF on when N limitation prevails (i.e., early in primary succession) and turn it off once N availability becomes sufficient (Fig. 1a). This type of response has been observed in boreal forests in Sweden, where BNF from cyanobacteria in feather mosses on the forest floor is low when soil N availability is high and vice versa (Zackrisson et al. 2004, DeLuca et al. 2007, 2008). However, ecosystems are typically not homogeneous, but rather are complex adaptive systems in which individuals are adapted to and interact with their local environments

Manuscript received 9 May 2008; revised 16 October 2008; accepted 20 October 2008; final version received 10 December 2008. Corresponding Editor: D. A. Wardle.

[1] E-mail: menge@nceas.ucsb.edu

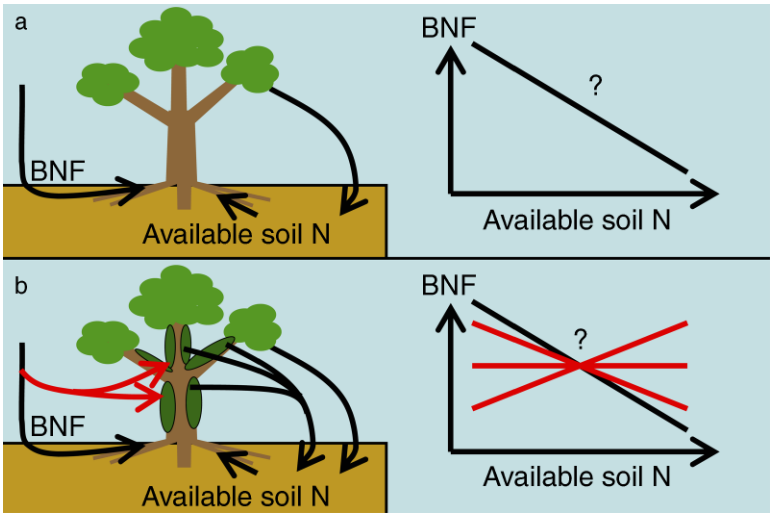

FIG. 1. Conceptual model of (a) a homogeneous ecosystem, in which soil nitrogen (N) determines what is available to the ecosystem vs. (b) a complex adaptive ecosystem, in which different ecosystem components such as soil-rooted plants and epiphytes have differential access to soil nutrients. In panel (a), N fixation is hypothesized to be a "nitrostat," providing a negative feedback to soil N availability, whereas it is unclear what the expected N fixation patterns are in panel (b). BNF is biological nitrogen fixation.

(Levin 1998). Therefore, spatial heterogeneity in the availability of N to organisms may influence BNF rates and may break the idealized dynamical nitrostat feedback. For example, nutrients available to N-fixing epiphytes include those running down tree branches or trunks, in bulk deposition, or in clouds and fog (but not in the soil), but when epiphytes die, their tissues can drop to the ground, ultimately increasing soil N availability. Therefore, some N fixers may not be ecosystem-level nitrostats, fixing N independently of, or even providing a positive feedback to, soil N availability (Fig. 1b). Understanding whether different N fixers act as nitrostats is essential to understanding nutrient dynamics over the course of ecosystem development, including how well ecosystems are buffered against perturbations (e.g., disturbance or fertilization) and to what extent BNF can bring ecosystems out of N limitation.

Despite the importance of BNF in succession and ecosystem development, we know relatively little about the dynamics of BNF and how it relates to N limitation. It is well documented that N-fixing angiosperms (hereafter, nodulating N fixers) often dominate early primary succession, but disappear during the course of succession in temperate and boreal forests (e.g., Wardle 1980, Binkley et al. 1992, Viereck et al. 1993, Walker 1993, Chapin et al. 1994). However, because there are few studies quantifying the amount of N (or even if) they fix through the course of succession, the dynamical pattern of the BNF process from nodulating N fixers, and its ecosystem-level imprint, is less clear.

Different dynamics would result from different BNF strategies, and two alternative BNF strategies in nodulating N fixers could produce fundamentally different ecosystem and community-level patterns. If nodulating N fixers are obligate, actively fixing N regardless of soil N availability, they would have an advantage early in succession when N is scarce, but as soil N builds up they might fix N even when they are no longer N-limited. This "over-fixation" could produce N-rich conditions for extended periods of time. Furthermore, over-fixation could contribute to their own exclusion, since BNF is energetically costly (Gutschick 1981), especially when limited by another resource (Vitousek and Field 1999, Rastetter et al. 2001), and could facilitate their competitors. A likely result of obligate BNF in nodulating N fixers would be a "poorly tuned" nitrostat that is controlled at the scale of community dynamics (species invasion and exclusion), resulting in a temporary buildup of N relative to other resources before nodulating N fixers are excluded.

Alternatively, if nodulating N fixers are facultative, decreasing BNF when N availability increases, they are less likely to over-fix. Facultative N fixers would therefore be less likely to produce N-rich conditions, and their absence from the community would not be as easily explained. Nodulating N fixers that are excluded during succession will act as a successional nitrostat regardless of whether they are facultative or obligate, but with critical differences in the timescale and effects on N dynamics. With facultative BNF, nodules have to be created or abandoned, a dynamic that is much faster than the exclusion of trees from a community, which is what turns off BNF in the obligate case. Therefore, facultative N fixers will likely produce much narrower swings in N availability.

Along with nodulating N fixers, many other organisms perform BNF in terrestrial ecosystems, including heterotrophic bacteria living in leaf litter (hereafter "litter"), cyanobacteria living in bryophyte mats (hereafter

"bryophytes"), and cyanolichens (hereafter "lichens"). The dynamics of BNF through primary succession and ecosystem development of these types, which live in different biogeochemical niches from soil-rooted plants, are even less clear than for nodulating N fixers. Bryophyte abundance and BNF seem to peak at intermediate-aged sites during long-term ecosystem development in Hawaii (Matzek and Vitousek 2003). Nitrogen-fixing lichens often successfully colonize early primary successional habitats, when available N is virtually absent (e.g., Chapin et al. 1994, Kurina and Vitousek 2001), but they are also often present and fixing N through long-term ecosystem development, along with bryophytes and litter (e.g., Crews et al. 2000, Matzek and Vitousek 2003). Since these other N fixers live in different biogeochemical niches, being spatially decoupled from the buildup of N in soils and lacking competitors who benefit directly from their BNF, these types may not be ecosystem-level nitrostats. Biological N fixation could therefore continue unimpeded over ecosystem development and could even provide a positive feedback to soil N availability if increasing soil N stimulates epiphytic BNF through some indirect mechanism (Fig. 1b).

In the present work we test three hypotheses about BNF dynamics in succession and long-term ecosystem development: (1) (a) Biological N fixation from nodulating N fixers decreases through succession and ecosystem development due to exclusion from the community (forming an ecosystem-level nitrostat), but (b) when nodulating N fixers are present their BNF rate is similar regardless of soil N conditions (consistent with obligate BNF). (2) Biological N fixation from lichens, bryophytes, and litter is non-nitrostatic, remaining constant with soil age and N conditions, because they are disconnected from the soil available N pool. (3) All BNF input sources are at least as important as atmospheric deposition. Potentially interesting BNF patterns would be irrelevant if their N input fluxes were negligible.

To test these three hypotheses, we quantified patterns of calibrated BNF and bulk N deposition at nine sites ranging in both age (from 7 to 120 000 yr old) and soil extractable inorganic N (from 3 to 35 mg N/kg) along the Franz Josef soil chronosequence in South Westland, New Zealand (Stevens 1968, Richardson et al. 2004). We present nitrogenase activity rates, densities, and BNF inputs for the *Coriaria arborea*/*Streptomyces* symbiosis (hereafter "*Coriaria*"), lichens, bryophytes, and litter.

Methods

Site descriptions

Recurring advances and retreats of the Franz Josef glacier (43°25′ S, 170°10′ E) have formed a chronosequence of schist-derived soils ranging from 0 yr old at the glacier terminal to >120 000 yr old near the coast (Stevens 1968, Almond et al. 2001, Richardson et al. 2004). We studied nine sites within 20 km of one another: 7, 60, 130, 280, 500, 5000, 12 000, 60 000, and 120 000 yr old in 2004. We sampled five circular 5 m radius subplots established by Richardson and colleagues (2004) at each site, except the 5000- and 12 000-yr-old sites where stakes could not be located. In these sites we arbitrarily determined subplot centers using spacing that was similar to other sites. Mean annual temperature is 10.8°C (Hessell 1982). Mean annual precipitation ranges from ~3500 mm at the three oldest sites to ~6500 mm at the six youngest sites (Richardson et al. 2004). We know of no large-scale disturbances since the time of formation listed for each site, hence we interpret the sites as primary successional. However, we cannot rule out the possibility that the older sites have experienced secondary disturbances, the potential effects of which on N dynamics could confound our interpretations.

Forty-five woody species have been recorded in the sites (Richardson et al. 2004), and there are many more herbaceous and bryophytic species. Canopy dominant trees are the N fixer *Coriaria* in the youngest sites (7 and 60 yr old, respectively), other evergreen angiosperms (*Metrosideros umbellata*, *Weinmannia racemosa*) in the intermediate-aged sites (130–500 yr old), and evergreen conifers (mostly *Dacrydium cupressinum*), along with *Metrosideros* and *Weinmannia* in the oldest sites (5000–120 000 yr old; Richardson et al. 2004). Other common trees and shrubs include *Griselinia littoralis*, *Aristotelia serrata*, various species of *Coprosma*, and the tree ferns *Dicksonia squarrosa* and *Cyathia smithii*. A full listing of woody species is in Richardson et al. (2004). There are many species of foliose lichens present in the sites, including *Pseudocyphellaria cinnamomea* (young to intermediate-aged sites), *P. homoeophylla* (most sites), *P. dissimilis* (intermediate sites), *Sticta* spp. (intermediate sites), *P. billardierei* (intermediate to old sites), and *P. faveolata* (intermediate to old sites). Bryophytes are similarly speciose, with the mosses *Ptychomnium aciculare* and *Hypnodendron* spp. and liverworts of the genus *Schistochila* abundant at most sites. These patterns are typical of New Zealand West Coast forests (Wardle 1980).

In many ways the Franz Josef chronosequence is similar to other well-studied chronosequences (e.g., Vitousek 2004, Wardle et al. 2004). Woody plant basal area (Wardle et al. 2004), maximum height, and diversity; soil available N (Richardson et al. 2004); and soil available P (Stevens 1968, Walker and Syers 1976, Richardson et al. 2004) increase through early primary succession, peak at intermediate-aged sites, and decline in older sites (but the available soil N:P ratio steadily increases). (See Table 1 for site details.) No fertilization studies have been performed, but the available data are consistent with N limitation early in succession and P limitation later on (Richardson et al. 2004).

Soil available N

Richardson et al. (2004) measured inorganic N mineralization rates in the top 10 cm of soil at each of these sites, and we use the N pool data they gathered to

TABLE 1. Selected vegetation and soil characteristics along the Franz Josef soil chronosequence (South Westland, New Zealand) from Richardson et al. (2004).

Site age (yr)	Maximum canopy height (m)	No. woody species	Inorganic N (mg/kg dry soil)	Inorganic P (mg/kg dry soil)	Organic P (mg/kg dry soil)	Soil pH
7	2	6	4	760	30	6.8
60	7	11	32	640	160	5.5
130	8	13	6	170	340	4.6
280	20	15	17	90	400	4.2
500	22	14	15	45	420	3.8
5000	24	17	35	35	310	3.8
12 000	35	15	21	25	260	3.8
60 000	25	14	7	15	180	3.8
120 000	12	11	5	5	100	3.9

Notes: With the exception of inorganic N, all data are approximate subplot medians. Inorganic N is the geometric mean of KCl-extracted NO_3-N + NH_4-N and is used in our analyses as available N.

construct these rates as our index of soil available N. They took five soil cores at each of the five subplots in each site, adjusted them to 60% water-holding capacity, moist-sieved them (4 mm), pooled them within each subplot, and performed 2 mol/L KCl extractions on 10 g (fresh mass) of soil at each site. They then measured NO_3-N and NH_4-N colorimetrically (QuikChem 8000, LaChat Instruments, Milwaukee, Wisconsin, USA) and presented data as mass N per mass dry soil. As shown in Table 1, soil inorganic N is very high at the 60-yr-old site, but aside from that it peaks at intermediate age. These patterns are similar to other measures of N availability such as aerobic mineralizable N and total soil N (Richardson et al. 2004), with the caveat that total soil N does not spike at the 60-yr-old site.

Rainwater collection

We installed three collectors (high-density polyethylene [HDPE] funnels 2 m off the ground, connected via silicone and Teflon tubing to dark HDPE bottles on the ground) for event-based bulk deposition sampling at open sites less than 800 m from the 7-, 12 000-, and 120 000-yr-old sites. Many of the nine sites are very close to one another, so three collectors were sufficient. No particles were found in collectors. We collected samples in winter (July and August) and summer (November and December), immediately filtering them to 45 μm and keeping them frozen from $\leq$6 h after collection until chemical analysis at Princeton. All materials were acid washed and/or thoroughly leached and were clean when tested for N contamination.

Rainwater N chemistry and fluxes

To analyze rainwater we used Alpkem colorimetry (OI Analytical, College Station, Texas, USA) for NH_4-N, Dionex ion chromatography (Bannockburn, Illinois, USA) for NO_3-N, and Shimadzu 5000 (Tokyo, Japan) 850°C platinum catalyst combustion for total dissolved N concentration ([TDN]). For methods details see Hedin et al. (2003). Total dissolved N concentration did not vary with event volume, season, or site, so we multiplied our global mean [TDN] by estimated annual rainfall at each collector site (Richardson et al. 2004) to estimate input fluxes. For sites lacking collectors, we used values from the climatically and spatially closest sites: the 7-yr-old site data for sites $\leq$5000 yr old, 12 000-yr-old site data for that site only, and 120 000-yr-old site data for sites $\geq$60 000 yr old.

Biological N fixation sample collection

When possible, samples were collected along randomly spaced and oriented transects. Otherwise (for rare types), samples were arbitrarily chosen from those available. *Coriaria* nodules were collected with >2 cm root tissue attached to allow carbon flow during incubation. Full depth profiles (on ground or epiphytic surface) of lichen, bryophyte, and litter samples of known area (typically 25 cm^2) were collected. These samples were not chosen for specific species, so in addition to the common species listed in the site description, many other species are represented in our acetylene reduction activity (ARA) and density sampling. Epiphytic samples were collected from <4 m height. Samples were weighed after incubation, then dried and weighed again for water content.

Nitrogenase activity rates

Nitrogenase activity rates were determined using the acetylene reduction assay (Hardy et al. 1968), which uses the fact that nitrogenase reduces acetylene (C_2H_2) to ethylene (C_2H_4). Within minutes of collection, samples were incubated at atmospheric pressure with 90% ambient air and 10% welding-grade C_2H_2 (BOC Gases, Auckland, New Zealand) in gas-tight, transparent half-pint canning jars, which were placed upside-down on the forest floor to simulate ambient light and temperature. Incubation periods were 30 min for *Coriaria* nodules and 24 h for other types, which were the minimum times needed to detect [C_2H_4] changes in winter; ARA was approximately linear over these timescales. Acetylene and sample blanks were used to correct for C_2H_4 contamination. Homogenized gas samples were stored in evacuated glass vials for fewer than seven days before [C_2H_4] analysis on an SRI 8610 gas chromatograph (SRI Instruments, Torrance, California, USA), using a Porapak N column (Alltech

Associates, Deerfield, Illinois, USA), ≥99.99% He as a carrier, and ≥99.99% H_2 combined with breathing air (BOC Gases) for combustion in the flame-ionization detector. Activity rates are expressed as micromoles C_2H_4 produced per hour of incubation time per gram of dry sample for nodules or nanomoles C_2H_4 per hour per square centimeter sample for other types. The minimum detection limit (MDL) was 0.024 nmol $C_2H_4 \cdot cm^{-2} \cdot h^{-1}$. Preliminary sampling showed that other sources thought to be important elsewhere (decomposing wood and epiphylls, e.g., Matzek and Vitousek 2003) were negligible sources of BNF here.

Nitrogen fixer densities

We determined dry mass of all *Coriaria* nodules found in 10 400-cm^2, ≥15 cm deep soil pits in each subplot. In each subplot, pits were evenly spaced along a randomly oriented pair of perpendicular transects. Nodule density estimates are conservative, as there may have been deeper nodules. To scale BNF rates by *Coriaria* density, we measured the circumference (at the base in the 7-yr-old site and at breast height in the 60-yr-old site) of each *Coriaria* stem.

Lichen densities were estimated by calibrated visual counts of lichen area (epiphytic and on the ground) divided by the ground area of each subplot. Bryophyte densities were estimated by percent cover of bryophytes on the ground and on each tree (multiplied by tree surface area) in each subplot. We estimated tree surface area by assuming trees are cylinders, multiplying circumference by height. Epiphytic estimates are lower bounds because we could not see high in the canopy (or on top of branches) and because our estimated allometries yield unrealistically low surface areas. Litter density was estimated by percent cover of litter on the ground.

Acetylene reduction to BNF conversion

We calibrated ARA to BNF using $^{15}N_2$ gas, conducting paired, simultaneous assays on fresh nodules, lichens, and bryophytes with C_2H_2 and $^{15}N_2$ in the field. Nodules were assayed for 1 h with 10% $^{15}N_2$ (≥98 atom %; Isotec, Miamisburg, Ohio, USA), lichens for 24 h with 10% $^{15}N_2$, and bryophytes for 24 h with 50% $^{15}N_2$. Litter was not calibrated because the incubation time necessary (>100 h) was beyond the range of linearity. Since our only data on free-living N fixers come from bryophytes, we used bryophyte conversion factors (CFs) to calibrate litter BNF. For $^{15}N_2$ assays we replaced the desired amount of gas with a mixture of $^{15}N_2$ (80%) and O_2 (20%). Incubations were terminated in the field by evacuating each jar (to >25 in Hg). Samples were removed from their vacuum at the field station, dried at 60°C, and stored dry until ground by roller mill or mortar and pestle. Ground, homogenized samples were analyzed for $^{15}N/^{14}N$ and percentage of N at the Boston University Stable Isotope Laboratory, Boston, Massachusetts, USA. The molar CF of ARA to BNF was calculated as (micromoles of C_2H_4 produced per hour per gram dry mass [DM] or square centimeter) divided by (micromoles N incorporated per hour per gram DM or square centimeter) divided by 2. All sampling took place between July 2004 and December 2005.

Biological nitrogen fixation input fluxes

For each season and each type of N fixer, BNF input fluxes were calculated as the product of ARA (in micromoles of C_2H_4 per hour per gram DM or square centimeter sample), density (in gram DM or square centimeter sample per square meter of ground), the reciprocal of the CF (in micromoles of C_2H_4 per micromole of N_2), and a unit conversion constant. For annual fluxes we assumed that summer and winter rates each occur for half the year.

Statistics

We used a maximum likelihood (ML) approach to analyze our data for three main reasons. First, because BNF is a product of three measured quantities (ARA, N fixer density, and CF), the estimated BNF inputs should incorporate error from all three sources. This error propagation, and the construction of confidence intervals that accompanies it, is not possible with classical statistics, but it is with ML. Second, some of our data were below the MDL of our analytical equipment. Traditional methods of dealing with this issue (such as treating all data points below the MDL as one-half the MDL) are inadequate, and ML allows a better treatment. Third, classical parametric statistics require certain assumptions (such as normality and homoscedasticity) that did not always fit our data, and ML is much more flexible in its assumptions. For example, ML allows variations on traditional tests, such as an ANOVA with nonnormally distributed residuals (Hilborn and Mangel 1997).

Our general statistical model assumes that each observation at site j and subplot i, O_{ij}, is given by a function of the independent variables (IVs), $f(\mathrm{IV})$, a random site effect, ε_j, and a random subplot effect, γ_i:

$$O_{ij} = f(\mathrm{IV}) + \varepsilon_j + \gamma_i. \quad (1)$$

The site and subplot effects are given by the probability distributions $P(\varepsilon_j)$ and $D(\gamma_i)$, which could be normal, gamma, or any other continuous distribution. The likelihood of a data set $\{O_1 \ldots O_N\}$ (with N data, indexed by k) given a model M is

$$\ell\{\{O_1 \ldots O_N\}|M\} = \begin{cases} \prod_{k=1}^{N} \int_{-\infty}^{\infty} [P(\varepsilon_j)D(\gamma_i)]d\varepsilon_j & \text{if } O_k \geq \mathrm{MDL} \\ \prod_{k=1}^{N} \int_{-\infty}^{\infty} \int_{-\infty}^{\mathrm{MDL}} [P(\varepsilon_j)D(\gamma_i)]dO_k d\varepsilon_j & \text{if } O_k < \mathrm{MDL} \end{cases} \quad (2)$$

where M describes the unique combination of the function $f(\mathrm{IV})$ and the probability distributions $P(\varepsilon_j)$

TABLE 2. Rainfall nutrient concentrations and inputs at three sites along the Franz Josef soil chronosequence.

Site	[NH_4-N] (μg N/L)	[NO_3-N] (μg N/L)	[TDN] (μg N/L)	Rainfall (mm/yr)	N input (kg N·ha^{-1}·yr^{-1})
1	7.69 (6.03–9.81)	9.24 (6.73–12.6)	18.7 (14.9–23.4)	6520	1.51 (1.31–1.74)
7	9.96 (8.10–12.2)	11.8 (8.71–15.9)	24.3 (19.5–30.2)	3706	0.86 (0.75–0.99)
9	6.10 (4.22–8.80)	15.6 (10.1–23.9)	28.5 (22.9–35.4)	3652	0.85 (0.74–0.97)

Notes: Concentration data are presented as geometric means (with SE bounds in parentheses), with $n = 14$ sampling dates for site 1, $n = 13$ for site 7, and $n = 12$ for site 9. Concentrations of each chemical species were statistically indistinguishable from site to site. The mean and SE for total dissolved nitrogen (TDN) data were used to calculate N input fluxes, assuming no uncertainty in rainfall flux. Rainfall fluxes are from Richardson et al. (2004).

and $D(\gamma_i)$ (and their parameters). The second case in Eq. 2 is for a datum below the MDL. In this case we do not know its true value, but we do know its likelihood (given the model M): the area under the probability density function up to the MDL.

The maximum likelihood is the global peak of Eq. 2 as a function of the model parameters, which we found on a computer with a peak-finding algorithm (simulated annealing) that reliably finds global maxima (Goffe et al. 1994). To determine which model fit best, e.g., whether a saturating increase in ARA as a function of soil age was better than a linear increase or no change with soil age, we compared many models against each other using the Akaike Information Criterion (AIC). More complicated models (those with more parameters) yield a higher maximum likelihood, but do not necessarily give better predictive power. The AIC balances this trade-off by assigning a penalty to each free parameter in the model. For confidence intervals (CIs) and error propagation, we again used simulated annealing to find the values that corresponded to half the χ^2 value for the number of free parameters (Hilborn and Mangel 1997). We present 68% CIs, which roughly correspond to the standard error (SE).

For density data, either soil age or soil inorganic N is the only IV, whereas for ARA, season (winter or summer) is also an IV. Our analysis of BNF inputs incorporates uncertainty from ARA, density, and CF data, and all BNF data are presented as means with 68% CIs. For bulk deposition data we used collector number (1, 2, or 3) and season as IVs and present the exact SE. Details of each analysis and additional explanations are in Appendix A.

RESULTS

Bulk deposition

Bulk deposition N concentrations ranged from below the MDL (1.0 μg/L) to 35.6 μg/L NH_4-N, 0.68 to 92.8 μg/L NO_3-N, and 2.48 to 107.7 μg/L TDN. Maximum likelihood analysis showed that all N species were best fit by models with the same mean and variance across sites and seasons except NO_3-N, which increased in winter. Means (SE bounds) were 7.81 (6.67–9.14) μg/L for NH_4-N, 11.7 (9.92–13.9) μg/L for NO_3-N, and 23.2 (20.2–26.7) μg/L TDN. Dissolved organic nitrogen (DON) (TDN − [NH_4-N + NO_3-N]) was negligible. Our estimated N deposition fluxes were 1.51, 0.85, and 0.86 kg N·ha^{-1}·yr^{-1} at the 7-, 12 000-, and 120 000-yr-old sites, respectively (Table 2). Although we only sampled across part of the annual cycle, our estimates are similar to global budget estimates for this region and other unpolluted temperate sites (1–2.5 kg N·ha^{-1}·yr^{-1}; Galloway et al. 2004).

Biological N fixation

Conversion factors.—Acetylene reduction activity to BNF CFs were 1.33 mol C_2H_4/mol N_2 for *Coriaria*, 1.58 mol C_2H_4/mol N_2 for lichens, and 0.25 mol C_2H_4/mol N_2 for bryophytes (Table 3). These are smaller than theoretical values (3.0 based on the number of electrons used to reduce C_2H_2 to C_2H_4 vs. N_2 to $2NH_3$ [Hardy et al. 1968] or 4.0 accounting for H_2 production [Rivera-Ortiz and Burris 1975, Simpson and Burris 1984]), but are within the range of empirical values for this method (Anderson et al. 2004). In particular, cyanobacteria in Norway have CFs of 0.02–0.48 (Liengen 1999), similar to our bryophytes.

Coriaria.—Nodule ARA rates ranged from 0.02 to 34.5 μmol C_2H_4·(g DM)$^{-1}$·h^{-1} and were best fit by a model with a seasonal effect on the mean, but without site or interaction effects on the mean or any effects on variance. The geometric means and 68% CIs across both sites were 3.73 (2.45–5.64) μmol C_2H_4·(g dry nodule)$^{-1}$·h^{-1} for summer and 0.55 (0.31–1.00) μmol C_2H_4·(g dry nodule)$^{-1}$·h^{-1} for winter (Fig. 2a). Nodule densities in individual subplots ranged from 0.025 to 16.1 g dry nodule/m^2, where each datum is the aggregation of 10 pits per subplot. Nodule density data were best fit by a model with the same mean and variance for both sites. The geometric mean and 68% CIs for both sites were 2.69 (1.51–4.68) g dry nodules/m^2 (Fig. 3a). We also calculated nodule densities per basal area of *Coriaria*, and the statistical results were the

TABLE 3. Empirically derived acetylene reduction activity (ARA) to N_2 fixation conversion factors, determined by paired ARA and $^{15}N_2$ incubations (mean with 68% CI in parentheses), in units of mol C_2H_4/mol N_2.

Substrate	Sample size	Conversion factor
Coriaria nodules	12	1.33 (1.15–1.56)
Cyanolichens	14	1.58 (1.18–1.76)
Bryophytes	10	0.25 (0.17–0.40)

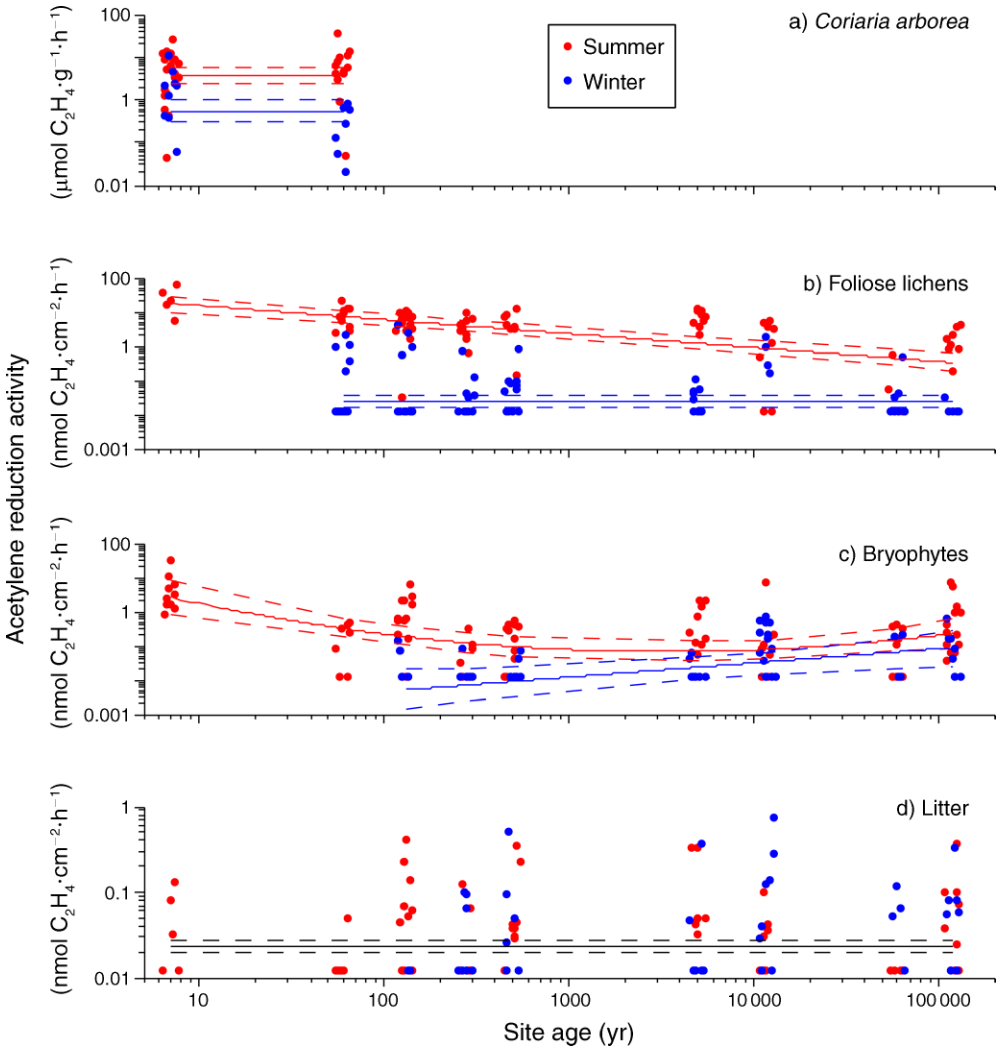

FIG. 2. Acetylene reduction activity: (a) *Coriaria arborea*, (b) foliose lichen, (c) bryophyte, and (d) litter acetylene reduction data are shown as a function of site age. Summer data are red, and winter data are blue. Although each datum comes from one of nine sites of discrete age, we have added a small random jitter to the horizontal value of each data point to improve readability of overlapping data. Data below the minimum detection limit are displayed as half this limit, but our statistical analyses do not make this assumption. Maximum likelihood estimates are shown as solid lines (in red and blue if there is a seasonal effect, otherwise in black), along with the 68% confidence interval of the mean (evaluated for each site age) in dashed lines of the same color. Units in panel (a) are micromoles of ethylene produced per gram of dry sample per hour, whereas units for panels (b)–(d) are nanomoles of ethylene produced per square centimeter of fresh sample per hour. Both axes are displayed on a logarithmic scale.

same: neither mean nor variance differed between the sites (data not shown).

Lichens.—Foliose lichens accounted for virtually all lichen BNF. Therefore, we do not present data from crustose or fruticose lichens, and hereafter we shorten "foliose lichen" to "lichen." Lichen ARA rates ranged from below the MDL to 61.5 nmol $C_2H_4 \cdot cm^{-2} \cdot h^{-1}$ and were best fit by a model with different seasonal patterns. Neither winter nor summer rates varied with soil inorganic N, nor did winter rates vary with soil age, but summer rates (higher than winter rates throughout) were best fit by an exponential decrease with soil age (Fig. 2b, Appendix B). Lichen density peaked in the intermediate-aged sites, with the highest densities of 0.05 m^2 lichen/m^2 ground between 130 and 5000 yr (Fig. 3b). As a function of soil inorganic N, lichen density was best fit by a saturating increase (Appendix C).

Bryophytes.—Bryophyte ARA rates tended to be lower than foliose lichen rates, although the range was similar: below the MDL to 30 nmol $C_2H_4 \cdot cm^{-2} \cdot h^{-1}$. The upper end of this range is an order of magnitude higher than the upper end of moss ARA rates measured in Sweden (Zackrisson et al. 2004, DeLuca et al. 2007, 2008), but most values are in the same range as those in Sweden and Hawaii (Matzek and Vitousek 2003). As with lichens and *Coriaria*, summer rates were higher than winter. The best-fit model for summer bryophyte ARA data increased at each end of the soil age/inor-

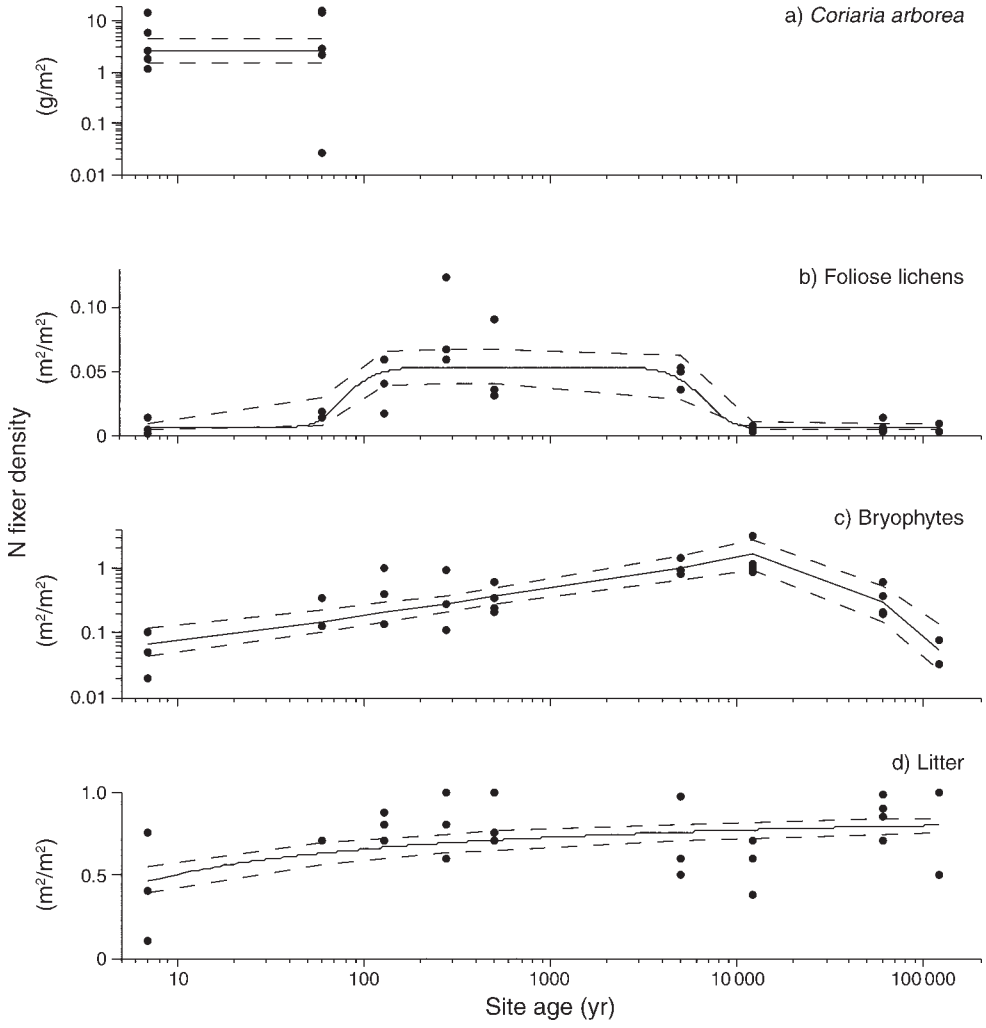

FIG. 3. Nitrogen (N) fixer density: (a) *Coriaria arborea*, (b) foliose lichen, (c) bryophyte, and (d) litter density data are shown as a function of site age. There are no seasonal differences for density, and there is no horizontal jitter added to the data points, but all other display attributes are the same as in Fig. 2. Units in panel (a) are grams of nodules per square meter of ground, whereas units for panels (b)–(d) are square meter of N fixer per square meter of ground. Note that the vertical axes for panels (a) and (c) and all horizontal axes are logarithmic.

ganic N spectrum with the highest values at the young/N-poor site. Winter data rose monotonically with soil age but remained constant with soil inorganic N (Fig. 2c, Appendix B). Bryophyte densities were more than an order of magnitude higher than foliose lichen densities and peaked at intermediate-aged sites. Bryophyte densities rose from 0.07 m^2 bryophyte/m^2 ground at the youngest site to a maximum of 1.6 m^2/m^2 at the 12 000-yr-old site (Fig. 3c). Bryophyte density increased as a saturating function of soil inorganic N (Appendix C).

Litter.—Litter ARA rates were similar to bryophyte and lichen winter rates (generally more than an order of magnitude lower than summer values), with a range of below the MDL to 0.75 nmol $C_2H_4 \cdot cm^{-2} \cdot h^{-1}$. In contrast to the other three classes, there was no seasonal difference in ARA rates. Litter ARA showed no pattern with soil age or soil inorganic N, with a mean of 0.024 nmol $C_2H_4 \cdot cm^{-2} \cdot h^{-1}$ (Fig. 2d, Appendix B). Litter density accumulated with soil age in a saturating manner (Fig. 3d), whereas it did not change with soil inorganic N (Appendix C).

Biological N fixation inputs.—Mean annual *Coriaria* BNF at both the 7- and 60-yr-old sites was 11 kg $N \cdot ha^{-1} \cdot yr^{-1}$ (Fig. 4a). Mean lichen BNF ranged from 0.02 to 2.0 kg $N \cdot ha^{-1} \cdot yr^{-1}$, with the highest rates at the 130–500-yr-old sites, reflecting the dominance of the density (peak-shaped) pattern over nitrogenase activity (decrease). Lichen BNF was also substantial (0.4–0.8 kg $N \cdot ha^{-1} \cdot yr^{-1}$) at the young sites and the 5000-yr-old site, but at the three oldest sites it was very low ($<$0.05 kg $N \cdot ha^{-1} \cdot yr^{-1}$; Fig. 4b). Mean bryophyte BNF ranged from 0.7 to 9.6 kg $N \cdot ha^{-1} \cdot yr^{-1}$ and showed peaks at both the 7- (9.6 kg $N \cdot ha^{-1} \cdot yr^{-1}$) and the 12 000-yr-old site (7.8 kg $N \cdot ha^{-1} \cdot yr^{-1}$; Fig. 4c). These peaks reflect

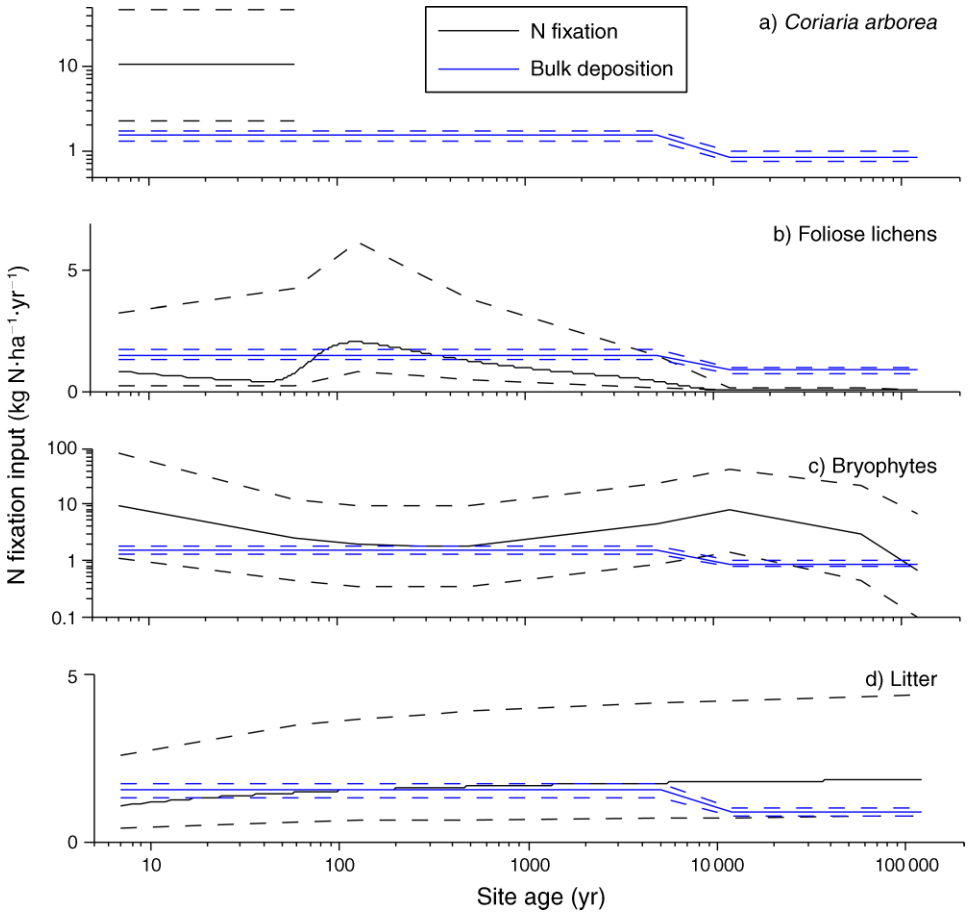

FIG. 4. Nitrogen (N) fixation inputs: the products for the means of the distributions of acetylene reduction activity, density, and the reciprocal of the conversion factor for (a) *Coriaria arborea*, (b) foliose lichens, (c) bryophytes, and (d) litter (using the bryophyte conversion factor) are shown as a function of site age. The 68% confidence intervals, which reflect uncertainty from acetylene reduction, density, and conversion factor data, are also shown as dashed lines. To calculate annual rates we averaged summer and winter values for acetylene reduction. As in Fig. 3, the vertical axes for panels (a) and (c) and all horizontal axes are logarithmic. The mean and 68% confidence intervals for bulk deposition N fluxes are also shown in blue.

substantial effects of both the density (peak-shaped) and nitrogenase patterns (highest at the youngest site, rising at both ends). The mean curve fit for bryophyte BNF approaches 20 kg N·ha^{-1}·yr^{-1} at 30 000 yr, but the fit is only relevant where we have sites, so 7.8 kg N·ha^{-1}·yr^{-1} at 12 000 yr is the relevant local maximum; only function values at ages of our sites are shown on Fig. 4c. Mean litter BNF ranged from 1.1 to 1.9 kg N·ha^{-1}·yr^{-1} and increased monotonically with soil age (Fig. 4d), reflecting the rise in litter density. For comparison, bulk deposition N inputs are also shown in Fig. 4. As a function of soil inorganic N, *Coriaria* BNF was the same at low and high values, lichen and bryophyte BNF increased, and litter BNF did not change (Fig. 5).

DISCUSSION

Relative importance of inputs from BNF vs. bulk N deposition

Our findings support the hypothesis that all sources of BNF at Franz Josef, individually, are at least as important as bulk deposition. Where present, *Coriaria* is at least tied as the largest N source, even though our estimates are at the lower end of the range of measured actinorhizal BNF inputs (Vitousek et al. 1987, Binkley et al. 1992, Cleveland et al. 1999, Uliassi and Ruess 2002). Bryophyte BNF is similarly important, rivaling *Coriaria* at the youngest site and exceeding all sources combined at the 5000–60 000-yr-old sites. Our bryophyte BNF estimates are larger than many reported values (Vitousek 1994, Crews et al. 2001, Matzek and Vitousek 2003, Zackrisson et al. 2004), reflecting all three data sources. At the youngest site, ARA rates are high but the density is low, whereas the opposite is true in intermediate-aged sites (Figs. 2c, 3c, 4c). The CF we measured is 12- to 16-fold lower than the theoretical value. Furthermore, our estimates of bryophyte BNF at intermediate-aged sites are underestimates, since we did not count bryophytes on top of canopy branches and all assays were performed on the canopy floor (where it was relatively dark). Compared to nodulated N fixers and

bryophytes, lichens and litter showed lower BNF rates, well within the ranges reported elsewhere (Sollins et al. 1980, Millbank 1981, Vitousek 1994, Cleveland et al. 1999, Crews et al. 2000, 2001, Kurina and Vitousek 2001, Matzek and Vitousek 2003, Antoine 2004). However, because they are similar in magnitude to bulk deposition and are more sustained throughout ecosystem development than *Coriaria* BNF, they too are important at many sites. As in the case of most studies of BNF in natural ecosystems, our estimates reveal substantial variability; any attempt to form a nutrient budget with our BNF data should therefore be done with caution.

Mechanisms of BNF dynamics at Franz Josef

The component and overall measures of *Coriaria* BNF, ARA (Fig. 2a), nodule mass (Fig. 3a), and total BNF (Fig. 4a), are indistinguishable at the 7- and 60-yr-old sites. This constancy is intriguing given the vast difference in N availability between these two sites (Fig. 5). The high N availability at the 60-yr-old site likely results from N-rich *Coriaria* litterfall (Richardson et al. 2004, 2005), but increased N availability does not decrease BNF. Across the natural range of N availability, *Coriaria* is an obligate N fixer, supporting our first hypothesis.

Coriaria is competitively excluded some time between the 60- and 130-yr-old sites, after one generation, mirroring the pattern of actinorhizal N fixers in temperate and boreal forests worldwide (Wardle 1980, Binkley et al. 1992, Viereck et al. 1993, Walker 1993, Chapin et al. 1994). At a timescale of a single generation of trees, *Coriaria* therefore acts as an ecosystem-level nitrostat, but the switching off of BNF is driven by exclusion from the community rather than a physiological response. This delay between increased soil N availability and turning off BNF therefore is a mechanism that can cause the rapid buildup of N-rich soil conditions.

Our findings raise a critical question: Why are nodulating N fixers excluded? Although a clear answer to this question is difficult without experiments, we can evaluate a number of potential explanations for the community-level exclusion of nodulating N fixers proposed in the literature. First, a trade-off between BNF and N use efficiency (NUE) can select against obligate N fixers (Menge et al. 2008), and NUE is substantially less in *Coriaria* (59 g biomass/g N) than in non-fixing angiosperms in the same sites (104 g biomass/g N) (Richardson et al. 2004, 2005). Second, preferential herbivory on obligate N fixers can select against N fixers (Vitousek and Field 1999, Menge et al. 2008); although we did not quantify herbivore damage, it appeared to be substantially greater on *Coriaria* than nearby non-fixing angiosperms (D. N. L. Menge, *personal observation*). Third, limitation by another resource can select against N fixers (Vitousek and Field 1999, Rastetter et al. 2001), and the high soil N availability at the 60-yr-old site (Richardson et al. 2004) indicates decreased N limitation

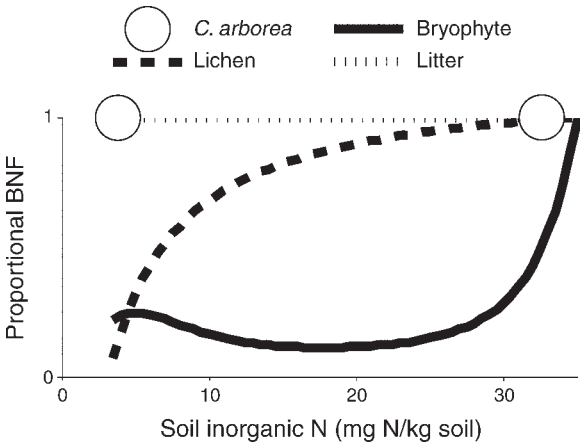

FIG. 5. Proportional biological nitrogen fixation (BNF) as a function of soil inorganic N. Nitrogen fixation trends reflect the product of acetylene reduction activity and density data sets using soil inorganic N (extractable $NO_3^- + NH_4^+$) and season as the independent variables, rather than soil age. Trends are shown as proportions of the maximum for each type, and all four types are shown. Two points only are shown for *Coriaria arborea*, rather than a continuous line.

(and probably limitation by another factor). Importantly, obligate BNF (Fig. 5) compounds the effective cost of limitation by another resource because resources spent on BNF (e.g., root tissue spent on nodules and photosynthate spent on feeding N-fixing symbionts) cannot be used to assimilate other resources.

In contrast to *Coriaria*, BNF from lichens, bryophytes, and litter persists throughout forest development at Franz Josef. Reflecting the lack of connection to the soil N pool, we show in Figs. 4 and 5 that BNF from these sources is not an ecosystem-level nitrostat, consistent with our second hypothesis. Surprisingly, however, BNF from (largely epiphytic) lichens and bryophytes increases with soil available N, providing a positive feedback to soil N (Figs. 4 and 5); this divergence from our hypothesis results primarily from changes in N fixer abundance.

This positive feedback between ecosystem-level N availability and epiphytic density (and thus total BNF) may stem from an indirect mechanism: When nutrients are readily available in the soil, plants grow taller and form a denser canopy, which provides more habitable surface area and increasingly moist conditions for epiphytes. However, since epiphytes are not connected to the soil pool, they maintain BNF regardless of soil N conditions, responding only to their local conditions (which may include throughfall N inputs, as has been shown in boreal forests in Sweden [DeLuca et al. 2008]). Given the large N input from bryophytes, this positive feedback to N availability in the soil could cause N-rich conditions, the extent of which would ultimately be limited by habitable epiphytic surface area. We speculate that this positive feedback mechanism of N richness may be important in wet regions worldwide.

Our findings point to two qualitatively different dynamics by which BNF can influence the long-term development of N cycling, each of which reflects a different biogeochemical niche (Fig. 1b). *Coriaria* appears to be a poorly tuned nitrostat at the ecosystem level, resulting from its community-level exclusion (which may in turn result from its obligate BNF). In contrast, bryophytes and lichens are a positive feedback to ecosystem N availability, with increased abundance and BNF in the fertile, intermediate-aged sites as tree biomass increases.

Broader implications of BNF patterns

Coupled with BNF data from other sites worldwide, our findings hint at fundamental global patterns of N dynamics. In primary successional and long-term chronosequences in Hawaiian tropical rain forests, lichen and bryophyte BNF also peaked in intermediate-aged sites. In support of our positive feedback idea, lichen and bryophyte BNF in Hawaii reflects a stronger influence of density than ARA patterns (Vitousek 1994, Crews et al. 2001, Matzek and Vitousek 2003). Decreases in epiphytic bryophyte and lichen density in old sites may ultimately result from P limitation (Benner and Vitousek 2007), but there is a period when N, P, and epiphytic surface area combine to allow substantial BNF. Aside from slight differences in relatively noisy litter BNF (which increased through early primary succession [Vitousek 1994, Crews et al. 2001] but decreased through long-term development [Crews et al. 2000] in Hawaii), the non-nitrostatic pattern of BNF from non-soil-rooted sources seems robust across taxa and biomes.

In nodulating N fixers, different strategies seem to operate in different biomes. *Coriaria* seems to be an obligate N fixer at Franz Josef, and other actinorhizal N fixers in the same early-successional niche in temperate and boreal forests also exhibit obligate BNF in the field. In successional forests in Oregon, Washington, and Alaska, *Alnus rubra* and *A. tenuifolia* fix N at similar rates (measured either directly, as here, or through accretion rates) in different periods of succession with drastically different soil N availability (Luken and Fonda 1983, Binkley et al. 1992, Uliassi and Ruess 2002). In stark contrast, leguminous trees that dominate tropical forests (including mature forests) seem to be facultative N fixers. *Acacia koa* in a Hawaiian plantation (Pearson and Vitousek 2001) and *Inga* spp. in the Barro Colorado National Monument, Panama (Barron 2007), seem to decrease BNF as soil N availability increases.

Coupled differences in BNF strategy and geographical distribution could help explain why nodulating N fixers are limited to successional forests in temperate and boreal zones but dominate mature tropical forests. Specifically, if temperate actinorhizal species incur the trade-off costs between BNF and other plant traits chronically, their fitness may be lower than non-fixers except in the most N-limited environments. Alternatively, if tropical leguminous N fixers can tune BNF rapidly, only fixing as much N as they need, they incur no net fitness cost relative to non-fixers, and do better on average because they fix N when it is beneficial. This difference in BNF strategy would also impact ecosystem-level N status in the two biomes.

Acknowledgments

We are greatly indebted to Sarah Richardson and Duane Peltzer for sharing soil extractable N data; Anna MacPherson and Jeremy Lichstein for field assistance; Sarah Richardson, Duane Peltzer, Margaret Barbour, and Troy Baisden for logistical help in New Zealand; Alex Barron, Megan McGroddy, and Melanie Vile for protocols and advice; and Steve Pacala for help with statistics. Sarah Batterman, Susana Bernal, Jack Brookshire, Jeanne DeNoyer, Stefan Gerber, Daniel Stanton, Nina Wurzburgur, and two anonymous reviewers provided comments that vastly improved the manuscript. This project was funded by a National Science Foundation Graduate Research Fellowship (to D. N. L. Menge), the National Science Foundation (DEB-0614116 and Doctoral Dissertation Improvement Grant DEB-0608267), and the Andrew W. Mellon Foundation Grant "The Emergence and Evolution of Ecosystem Functioning."

Literature Cited

Almond, P. C., N. T. Moar, and O. B. Lian. 2001. Reinterpretation of the glacial chronology of South Westland, New Zealand. New Zealand Journal of Geology and Geophysics 44:1–15.

Anderson, M. D., R. W. Ruess, D. D. Uliassi, and J. S. Mitchell. 2004. Estimating N_2 fixation in two species of *Alnus* in interior Alaska using acetylene reduction and $^{15}N_2$ uptake. Ecoscience 11:102–112.

Antoine, M. E. 2004. An ecophysiological approach to quantifying nitrogen fixation by *Lobaria oregana*. Bryologist 107:82–87.

Barron, A. R. 2007. Patterns and controls on nitrogen fixation in a lowland tropical forest, Panama. Dissertation. Princeton University, Princeton, New Jersey, USA.

Benner, J. W., and P. M. Vitousek. 2007. Development of a diverse epiphyte community in response to phosphorus fertilization. Ecology Letters 10:628–636.

Binkley, D., P. Sollins, R. Bell, D. Sachs, and D. Myrold. 1992. Biogeochemistry of adjacent conifer and alder–conifer stands. Ecology 73:2022–2033.

Chapin, F. S. I., L. R. Walker, C. L. Fastie, and L. C. Sharman. 1994. Mechanisms of primary succession following deglaciation at Glacier Bay, Alaska. Ecological Monographs 64: 149–175.

Cleveland, C. C., A. R. Townsend, D. S. Schimel, H. Fisher, R. W. Howarth, L. O. Hedin, S. S. Perakis, E. F. Latty, J. C. Von Fischer, A. Elseroad, and M. F. Wasson. 1999. Global patterns of terrestrial biological nitrogen (N_2) fixation in natural ecosystems. Global Biogeochemical Cycles 13:623–645.

Crews, T. E., H. Farrington, and P. M. Vitousek. 2000. Changes in asymbiotic, heterotrophic nitrogen fixation on leaf litter of *Metrosideros polymorpha* with long-term ecosystem development in Hawaii. Ecosystems 3:386–395.

Crews, T. E., L. M. Kurina, and P. M. Vitousek. 2001. Organic matter and nitrogen accumulation and nitrogen fixation during early ecosystem development in Hawaii. Biogeochemistry 52:259–279.

DeLuca, T. H., O. Zackrisson, F. Gentili, A. Sellstedt, and M. C. Nilsson. 2007. Ecosystem controls on nitrogen fixation in boreal feather moss communities. Oecologia 152:121–130.

DeLuca, T. H., O. Zackrisson, M. J. Gundale, and M. C. Nilsson. 2008. Ecosystem feedbacks and nitrogen fixation in boreal forests. Science 320:1181–1181.

Galloway, J. N., et al. 2004. Nitrogen cycles: past, present, and future. Biogeochemistry 70:153–226.
Goffe, W. L., G. D. Ferrier, and J. Rogers. 1994. Global optimization of statistical functions with simulated annealing. Journal of Econometrics 60:65–99.
Gutschick, V. P. 1981. Evolved strategies in nitrogen acquisition by plants. American Naturalist 118:607–637.
Hardy, R. W. F., R. D. Holsten, B. K. Jackson, and R. C. Burns. 1968. The acetylene-ethylene assay for N_2-fixation: laboratory and field evaluation. Plant Physiology 43:1185–1207.
Hedin, L. O., P. M. Vitousek, and P. A. Matson. 2003. Nutrient losses over four million years of tropical forest development. Ecology 84:2231–2255.
Hessell, J. W. D. 1982. The climate and weather of Westland, New Zealand. Meteorological Service Miscellaneous Publications 115:1–44.
Hilborn, R., and M. Mangel. 1997. The ecological detective: confronting models with data. Princeton University Press, Princeton, New Jersey, USA.
Kurina, L. M., and P. M. Vitousek. 2001. Nitrogen fixation rates of *Stereocaulon vulcani* on young Hawaiian lava flows. Biogeochemistry 55:179–194.
Levin, S. A. 1998. Ecosystems and the biosphere as complex adaptive systems. Ecosystems 1:431–436.
Liengen, T. 1999. Conversion factor between acetylene reduction and nitrogen fixation in free-living cyanobacteria from high arctic habitats. Canadian Journal of Microbiology 45: 223–229.
Luken, J. O., and R. W. Fonda. 1983. Nitrogen accumulation in a chronosequence of red alder communities along the Hoh River, Olympic National Park, Washington. Canadian Journal of Forest Research 13:1228–1237.
Matzek, V., and P. M. Vitousek. 2003. Nitrogen fixation in bryophytes, lichens, and decaying wood along a soil–age gradient in Hawaiian montane rain forest. Biotropica 35:12–19.
Menge, D. N. L., S. A. Levin, and L. O. Hedin. 2008. Evolutionary trade-offs can select against nitrogen fixation and thereby maintain nitrogen limitation. Proceedings of the National Academy of Sciences (USA) 105:1573–1578.
Millbank, J. W. 1981. The assessment of nitrogen fixation and throughput by lichens: I. The use of a controlled environment chamber to relate acetylene reduction estimates to nitrogen fixation. New Phytologist 89:647–655.
Pearson, H. L., and P. M. Vitousek. 2001. Stand dynamics, nitrogen accumulation, and symbiotic nitrogen fixation in regenerating stands of *Acacia koa*. Ecological Applications 11:1381–1394.
Rastetter, E. B., P. M. Vitousek, C. B. Field, G. R. Shaver, D. A. Herbert, and G. I. Agren. 2001. Resource optimization and symbiotic nitrogen fixation. Ecosystems 4:369–388.
Richardson, S. J., D. A. Peltzer, R. B. Allen, and M. S. McGlone. 2005. Resorption proficiency along a chronosequence: responses among communities and within species. Ecology 86:20–25.
Richardson, S. J., D. A. Peltzer, R. B. Allen, M. S. McGlone, and R. L. Parfitt. 2004. Rapid development of phosphorus limitation in temperate rainforest along the Franz Josef soil chronosequence. Oecologia 139:267–276.
Rivera-Ortiz, J. M., and R. H. Burris. 1975. Interactions among substrates and inhibitors of nitrogenase. Journal of Bacteriology 123:537–545.
Simpson, F. B., and R. H. Burris. 1984. A nitrogen pressure of 50 atmospheres does not prevent evolution of hydrogen by nitrogenase. Science 224:1095–1097.
Sollins, P., C. C. Grier, F. M. McCorison, K. Cromack, and R. Fogel. 1980. The internal element cycles of an old-growth Douglas-fir ecosystem in western Oregon. Ecological Monographs 50:261–285.
Stevens, P. R. 1968. A chronosequence of soils near the Franz Josef Glacier. University of Canterbury, Christchurch, New Zealand.
Uliassi, D. D., and R. W. Ruess. 2002. Limitations to symbiotic nitrogen fixation in primary succession on the Tanana River floodplain. Ecology 83:88–103.
Viereck, L. A., C. T. Dyrness, and M. J. Foote. 1993. An overview of the vegetation and soils of the floodplain ecosystems of the Tanana River, interior Alaska. Canadian Journal of Forest Research 23:889–898.
Vitousek, P. M. 1994. Potential nitrogen fixation during primary succession in Hawaii Volcanoes National Park. Biotropica 26:234–240.
Vitousek, P. M. 2004. Nutrient cycling and limitation: Hawai'i as a model system. Princeton University Press, Princeton, New Jersey, USA.
Vitousek, P. M., and C. B. Field. 1999. Ecosystem constraints to symbiotic nitrogen fixers: a simple model and its implications. Biogeochemistry 46:179–202.
Vitousek, P. M., L. R. Walker, L. D. Whiteaker, D. Mueller-Dombois, and P. A. Matson. 1987. Biological invasion by *Myrica faya* alters ecosystem development in Hawaii. Science 238:802–804.
Walker, L. R. 1993. Nitrogen fixers and species replacements in primary succession. Pages 249–272 *in* J. Miles and D. W. H. Walton, editors. Primary succession on land. Blackwell Scientific, Oxford, UK.
Walker, T. W., and J. K. Syers. 1976. The fate of phosphorus during pedogenesis. Geoderma 15:1–19.
Wardle, D. A., L. R. Walker, and R. D. Bardgett. 2004. Ecosystem properties and forest decline in contrasting long-term chronosequences. Science 305:509–513.
Wardle, P. 1980. Primary succession in Westland National Park and its vicinity, New Zealand. New Zealand Journal of Botany 18:221–232.
Zackrisson, O., T. H. DeLuca, M.-C. Nilsson, A. Sellstedt, and L. M. Berglund. 2004. Nitrogen fixation increases with successional age in boreal forests. Ecology 85:3327–3334.

APPENDIX A

Derivation and details of maximum-likelihood statistics (*Ecological Archives* E090-153-A1).

APPENDIX B

Acetylene reduction activity as a function of soil available nitrogen (*Ecological Archives* E090-153-A2).

APPENDIX C

Nitrogen fixer density as a function of soil available nitrogen (*Ecological Archives* E090-153-A3).

Ecological Archives **E090-153-A1**

Duncan N. L. Menge and Lars O. Hedin. 2009. Nitrogen fixation in different biogeochemical niches along a 120000-year chronosequence in New Zealand. *Ecology* 90:2190–2201.

Appendix A. Derivation and details of maximum-likelihood statistics.

Likelihood derivation

The general structure of our data is that each observation, O_{ij}, is given by a function of the independent variables (the base 10 logarithm of soil age for most data as well as season for ARA data), a random site effect, and a random subplot effect. Here we call the function $f(A_j)$ to indicate that it is a function of the age A of site j, the site effect ε_j, and the subplot effect γ_i:

$$O_{ij} = f(A_j) + \varepsilon_j + \gamma_i. \quad \text{(A.1)}$$

ε_j is pulled from the probability density function $P(\varepsilon_j)$, and γ_i from $D(\gamma_i)$, both with mean 0. Since we have a sum of two random variables, a convolution integral over ε_j gives the likelihood. There are m sites, indexed by j, and n_j subplots in each site, indexed by i, for a total of N data, indexed by k (which will hereafter replace ij for brevity). Therefore, the likelihood of a particular dataset $\{O_1 \ldots O_N\}$ given a particular model M is

$$\ell\left\{\{O_1 \ldots O_N\}\,|M\right\} = \begin{cases} \prod_{k=1}^{N} \int_{-\infty}^{\infty} \left[P\left(\varepsilon_j\right) D\left(\gamma_i\right)\right] d\varepsilon_j & \text{if } O_k \geq \text{MDL} \\ \prod_{k=1}^{N} \int_{-\infty}^{\infty} \int_{-\infty}^{\text{MDL}} \left[P\left(\varepsilon_j\right) D\left(\gamma_i\right)\right] dO_k d\varepsilon_j & \text{if } O_k < \text{MDL} \end{cases} \quad \text{(A.2)}$$

The model M describes the unique combination of a function $f(A_j)$ and the probability density functions $P(\varepsilon_j)$ and $D(\gamma_i)$.

If a datum is below the minimum detection limit (MDL) we do not know its value, but only that it lies below the MDL, so the likelihood of a datum below the MDL is the integral over O_k up to the MDL. This second case is only relevant for data that have a MDL, such as ARA. To show our solutions for Eq. A.2 we use the example of Gaussian distributions for $P(\varepsilon_j)$ and $D(\gamma_i)$; the variations thereon use similar calculations.

With means 0 and standard deviations σ and $\sigma\beta$ for $P(\varepsilon_j)$ and $D(\gamma_i)$,

$$\ell\left\{\{O_1 \ldots O_N\}\,|M\right\} = \begin{cases} \prod_{k=1}^{N} \int_{-\infty}^{\infty} g(O_k, \varepsilon_j) d\varepsilon_j & \text{if } O_k \geq \text{MDL} \\ \prod_{k=1}^{N} \int_{-\infty}^{\infty} \int_{-\infty}^{\text{MDL}} g(O_k, \varepsilon_j) dO_k d\varepsilon_j & \text{if } O_k < \text{MDL} \end{cases} \quad \text{(A.3)}$$

$$g(O_k, \varepsilon_j) = \frac{1}{\sigma\sqrt{2\pi}} exp\left(\frac{-\varepsilon_j^2}{2\sigma^2}\right) \frac{1}{\sigma\beta\sqrt{2\pi}} exp\left(\frac{-\left(O_k - f(A_j) - \varepsilon_j\right)^2}{2\sigma^2\beta^2}\right) \quad \text{(A.4)}$$

With a bit of algebra Eq. A.3 can be rearranged to

$$\ell\left\{\{O_1 \ldots O_N\}\,|M\right\} = \begin{cases} \prod_{k=1}^{N} \dfrac{exp\left(\dfrac{-\left(O_k - f(A_j)\right)^2}{2\sigma^2(\beta^2+1)}\right) \int_{-\infty}^{\infty} h(O_k,\varepsilon_j)d\varepsilon_j}{\sigma^2\beta 2\pi} & \text{if } O_k \geq \text{MDL} \\ \prod_{k=1}^{N} \dfrac{\int_{-\infty}^{\text{MDL}} exp\left(\dfrac{-\left(O_k - f(A_j)\right)^2}{2\sigma^2(\beta^2+1)}\right) \int_{-\infty}^{\infty} h(O_k,\varepsilon_j)d\varepsilon_j dO_k}{\sigma^2\beta 2\pi} & \text{if } O_k < \text{MDL} \end{cases} \quad \text{(A.5)}$$

$$h(O_k,\varepsilon_j) = exp\left(\frac{-\left(\varepsilon_j - \frac{O_k - f(A_j)}{\beta^2+1}\right)^2}{\frac{2\sigma^2\beta^2}{\beta^2+1}}\right) \quad \text{(A.6)}$$

$h(O_k,\varepsilon_j)$ is the exponential part of a Gaussian probability density function with standard deviation $\sigma\beta/\sqrt{(\beta^2+1)}$, so it is equal to $\sqrt{(2\pi)}\sigma\beta/\sqrt{(\beta^2+1)}$, and thus, if we let $s = \sigma\sqrt{(\beta^2+1)}$ Eq. A.5 reduces to

$$\ell\left\{\{O_1 \ldots O_N\}\,|M\right\} = \begin{cases} \prod_{k=1}^{N} \dfrac{exp\left(\dfrac{-\left(O_k - f(A_j)\right)^2}{2s^2}\right)}{\sqrt{2\pi s^2}} & \text{if } O_k \geq \text{MDL} \\ \prod_{k=1}^{N} \dfrac{\int_{-\infty}^{\text{MDL}} exp\left(\dfrac{-\left(O_k - f(A_j)\right)^2}{2s^2}\right) dO_k}{\sqrt{2\pi s^2}} & \text{if } O_k < \text{MDL} \end{cases} \quad \text{(A.7)}$$

Computing log likelihoods is faster than likelihoods, so we take the log of Eq. A.7:

$$\mathbf{L}\{\{O_1 \ldots O_N\}|M\} = \begin{cases} \sum_{k=1}^{N} \frac{-(O_k - f(A_j))^2}{2s^2} - \frac{ln(2\pi s^2)}{2} & \text{if } O_k \geq \text{MDL} \\ \sum_{k=1}^{N} ln\left(\frac{\int_{-\infty}^{\text{MDL}} exp\left(\frac{-(O_k - f(A_j))^2}{2s^2}\right) dO_k}{\sqrt{2\pi s^2}}\right) & \text{if } O_k < \text{MDL} \end{cases} \quad (A.8)$$

For datasets that do not have an MDL, we can constrain s^2 analytically. Differentiating the first case with respect to s^2 and setting equal to zero (which must be true for **L** to be maximized) yields

$$s^2 = \frac{\sum_{k=1}^{N} (O_k - f(A_j))^2}{N}. \quad (A.9)$$

Eq. A.8 (and plugging Eq. A.9 into Eq. A.8 where applicable) is the calculation we perform with the computer. The computer program (in C, available from the corresponding author upon request) jumps around in parameter space, computes the likelihood for each parameter set, and accepts the new parameter set if it either yields a greater likelihood than the last (with probability 1) or a lesser likelihood than the last (with probability slightly greater than 0). Accepting a new parameter set that yields a lesser likelihood prevents the algorithm from becoming stuck on local peaks in parameter space. For each model the program runs ten times from different starting points to ensure the algorithm converges on the same maximum, and for each run the program takes 120,000 jumps in parameter space. We compared multiple models against each other, and accepted the model with the lowest Akaike Information Criterion (which equals the opposite of the maximum log likelihood plus 2 times the number of free parameters).

Each dataset had a unique set of models we compared, explained in the following sections.

Models

Coriaria arborea

For *Coriaria* we only have data from two sites (7 and 60 y.o.), so instead of a function of age or soil inorganic N we use an ANOVA-like test. For nodule density we assume residuals are lognormally distributed, and for nodule density per basal area we assume they are normally distributed. We then compare models with the same mean and variance across the two sites, a different mean but the same variance, the same mean but a different variance, and different means and variances. The datasets for both nodule density and nodule density per basal area were best fit by a model with the same mean and variance for both sites. We assumed nodule ARA data were lognormally distributed. We tested for a seasonal effect α, a site effect β, and an interaction term γ by comparing all subsets of the following function:

$$f(A_j, S) = \mu + \alpha + \beta + \gamma \quad (A.10)$$

Nodule ARA data were best fit by a model with a seasonal effect α but no site or interaction effects. For nodule conversion factor data we assumed lognormally distributed residuals, and applied the same mean to data from all sites (and both seasons, since conversion factors were only measured during the summer).

Foliose lichens

For foliose lichen density we assumed that the residuals were normally distributed, but that the spread within the site increases with the mean; i.e. we assumed a constant coefficient of variation. The functions of age or soil inorganic N we compared were all subsets of the following functions:

$$f(A_j) = c_1 + c_2 A_j + c_3 A_j^2 + c_4 A_j^3 \quad (A.11)$$

$$f(A_j) = c_1 + c_2 e^{-\frac{|A_j - c_3|^{c_4}}{c_5^{c_4}} + c_6 A_j} \quad (A.12)$$

$$f(A_j) = c_1 + \frac{c_2 A_j}{c_3 + A_j} \quad (A.13)$$

For soil age, the data were best fit by a hump-shaped model with no skew,

$$f(A_j) = c_1 + c_2 e^{-|A_j - c_3|^{c_4}}, \quad (A.14)$$

whereas for soil inorganic N, the data were best fit by a saturating curve,

$$f(A_j) = c_1 + \frac{c_2 A_j}{c_3 + A_j} \quad (A.15)$$

For foliose lichen ARA data we assumed lognormally distributed residuals. The functions we tried were all possible subsets of the following, allowing for different functions for winter and summer data:

$$f(A_j) = c_1 + c_2 A_j + c_3 A_j^2 + c_4 A_j^3 \quad (A.16)$$

$$f(A_j) = c_1 + \frac{c_2 A_j}{c_3 + A_j} \quad (A.17)$$

For soil age, the foliose lichen ARA data were best fit by a model with different functions for different seasons: a constant value for the winter data, and a linear decreasing function for summer data. For soil inorganic N, the foliose lichen ARA data were best fit by a model with different functions for different seasons, where both were constant (and summer was greater than winter).

For foliose lichen conversion factor data we assumed lognormally distributed residuals, and applied the same mean to data from all sites (and both seasons, since conversion factors were only measured during the summer).

Bryophytes

For bryophyte density data we assumed lognormally distributed residuals. The functions of age we tried we all possible subsets of the following:

$$f(A_j) = c_1 + c_2 A_j + c_3 A_j^2 + c_4 A_j^3 + c_5 e^{\frac{-|A_j - c_6|^{c_7}}{c_8^{c_7}} + c_9 A_j + c_1 0} \quad (A.18)$$

$$f(A_j) = c_1 + \frac{c_2 A_j}{c_3 + A_j} \quad (A.19)$$

The best model for soil age was a hump-shaped function with skew,

$$f(A_j) = c_1 e^{\frac{-|A_j - c_2|}{c_3} + c_4 A_j}, \quad (A.20)$$

and the best model for soil inorganic N was a saturating increase,

$$f(A_j) = \frac{c_1 A_j}{c_2 + A_j}. \quad (A.21)$$

For bryophyte ARA we assumed lognormally distributed residuals. The functions we tried were all possible subsets of the following, allowing for different functions for winter and summer data:

$$f(A_j) = c_1 + c_2 A_j + c_3 A_j^2 + c_4 A_j^3 \quad (A.22)$$

$$f(A_j) = c_1 + \frac{c_2 A_j}{c_3 + A_j} \quad (A.23)$$

For soil age, bryophyte ARA data were best fit by a model with different winter and summer functions: a rising linear function for winter data and an upward-curving quadratic function for summer data. For soil inorganic N, bryophyte ARA data were best fit by a model with different winter and summer functions: a constant for winter data and an upward-curving quadratic function for summer data.

For bryophyte conversion factor we assumed lognormally distributed residuals, and applied the same mean to data from all sites (and both seasons, since conversion factors were only measured during the summer).

Litter

For litter density data we assumed normally distributed residuals. The functions we tried for $f(A_j)$ were all possible subsets of a saturating curve with an intercept,

$$f(A_j) = c_1 + \frac{c_2 A_j}{c_3 + A_j}. \quad (A.24)$$

The best fit model for soil age was a saturating curve without an intercept, and for soil inorganic N was a constant.

For litter ARA data we assumed lognormally distributed residuals, and tried all possible subsets of the following functions on all the data, with and without the possibility of different functions for summer and winter data:

$$f(A_j) = c_1 + c_2 A_j + c_3 A_j^2 + c_4 A_j^3 \quad (A.25)$$

$$f(A_j) = c_1 + \frac{c_2 A_j}{c_3 + A_j} \quad (A.26)$$

Litter ARA data were best fit by a model with no age or season effects for both soil age and inorganic N.

Bulk deposition nutrient concentrations

We assumed that bulk deposition NH_4^+, NO_3^-, and TDN data were lognormally distributed. There were three collectors, so we compared models similar to those for nodule data: with the same or different means and variances across sites and seasons.

For all N species the data were best fit by a model with the same mean and variance across sites, except NO_3^-, which had a significant seasonal effect on the mean with lower concentrations in summer.

[Back to E090-153]

Ecological Archives E090-153-A2

Duncan N. L. Menge and Lars O. Hedin. 2009. Nitrogen fixation in different biogeochemical niches along a 120000-year chronosequence in New Zealand. *Ecology* 90:2190–2201.

Appendix B. A figure showing acetylene reduction activity as a function of soil available nitrogen.

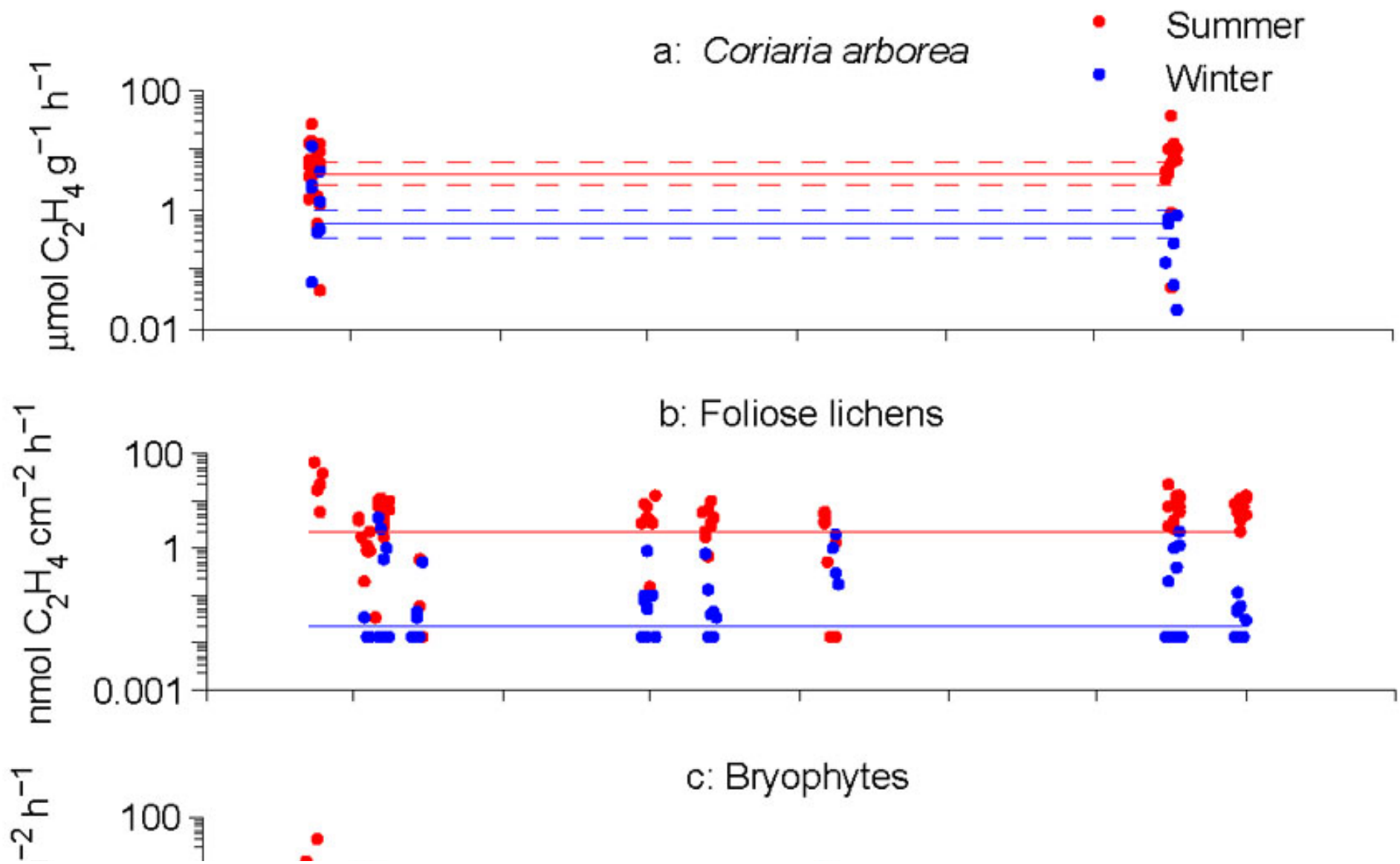

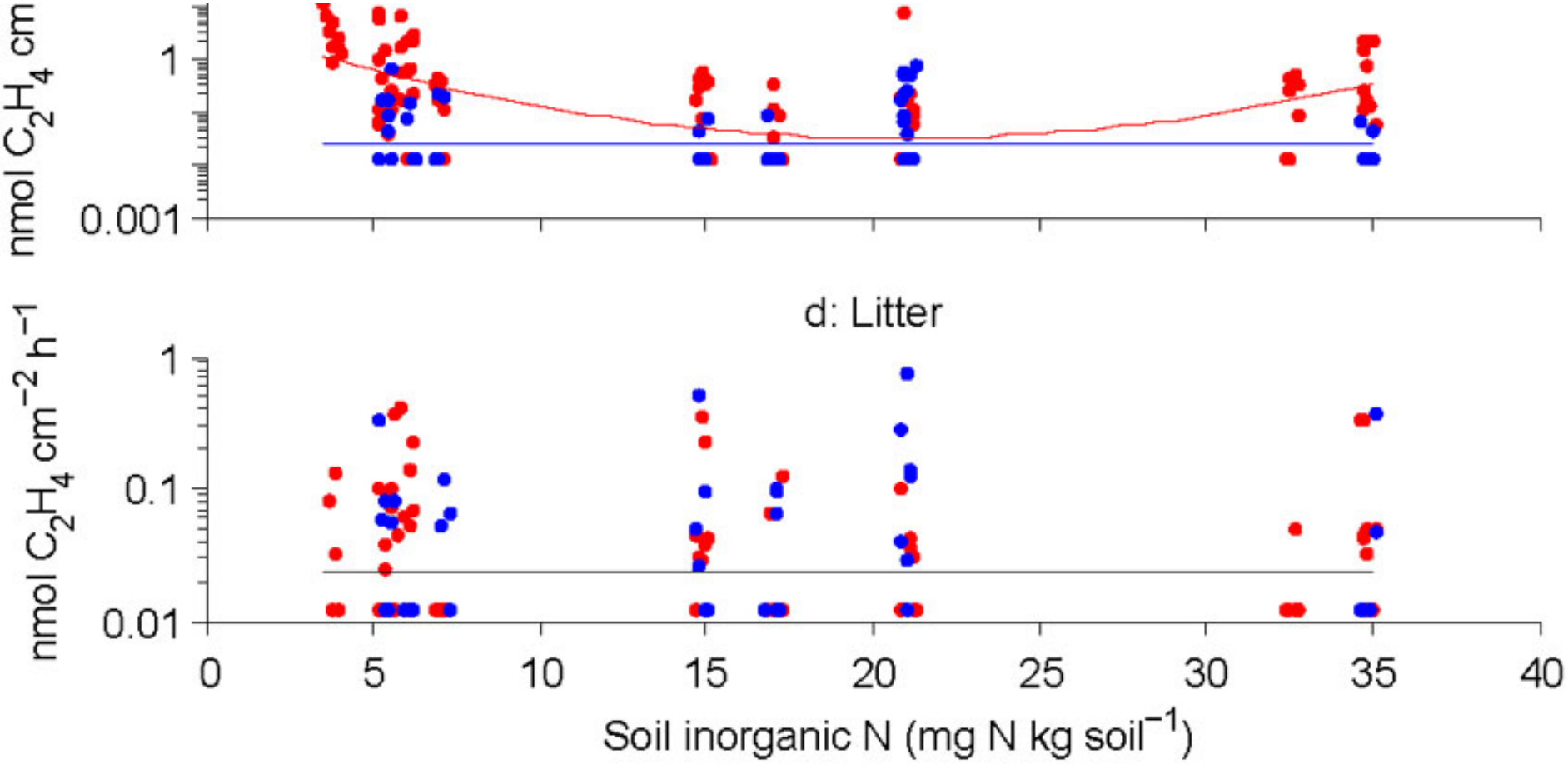

FIG. B1. Caption: (a) *Coriaria arborea*, (b) foliose lichen, (c) bryophyte, and (d) litter acetylene reduction activity are shown as a function of soil inorganic nitrogen availability across the Franz Josef chronosequence. As in Fig. 2, summer data are red, winter data are blue, and we have added a small random horizontal jitter to each datapoint to improve readability of overlapping data. Also as in Fig. 2, data below the minimum detection limit are displayed as half this limit, but our maximum likelihood estimates - shown in solid lines - do not make this assumption (see main text and Appendix A). Note that the units of (a) differ from (b)–(d). As in Fig. 2, the vertical axes are displayed on a logarithmic scale, but unlike Fig. 2, the horizontal axes are displayed on a linear scale.

[Back to E090-153]

Ecological Archives E090-153-A3

Duncan N. L. Menge and Lars O. Hedin. 2009. Nitrogen fixation in different biogeochemical niches along a 120000-year chronosequence in New Zealand. *Ecology* 90:2190–2201.

Appendix C. A figure showing nitrogen fixer density as a function of soil available nitrogen.

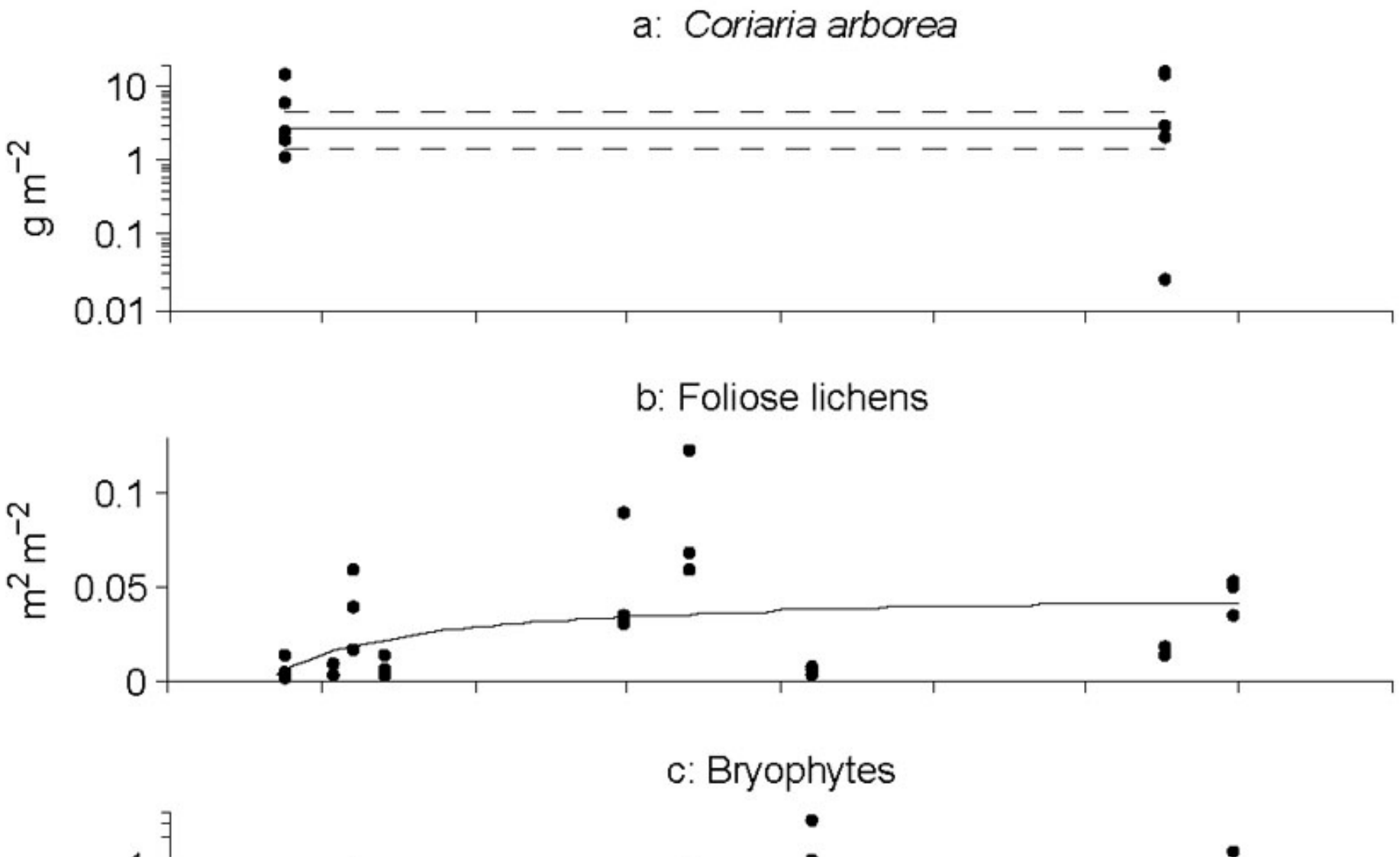

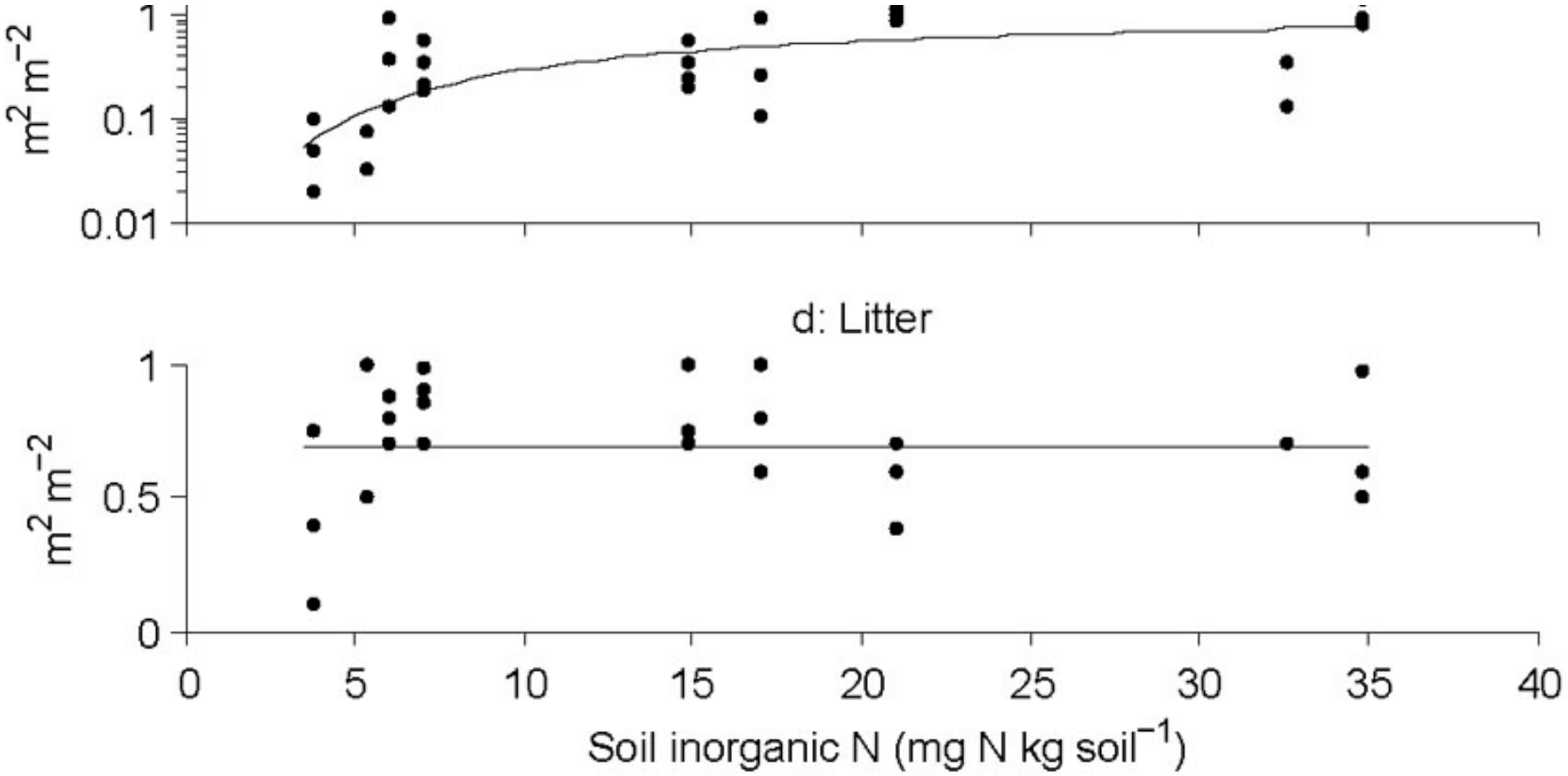

FIG. C1. Caption: (a) *Coriaria arborea*, (b) foliose lichen, (c) bryophyte, and (d) litter densities are shown as a function of soil inorganic nitrogen availability across the Franz Josef chronosequence. As in Fig. 3, there is no distinction between summer and winter data, and there is no jitter added. As in other figures, maximum-likelihood estimates are displayed in solid lines. As in Fig. 3, the units of (a) differ from (b)–(d), and the vertical axes of (a),(c) are displayed on a logarithmic scale, whereas the vertical axes of (b),(d) are displayed on a linear scale. Unlike Fig. 3, the horizontal axes are displayed on a linear scale.

[Back to E090-153]